



1 **Energy states of soil water – a thermodynamic perspective on**
2 **storage dynamics and the underlying controls**

3
4 Erwin Zehe¹, Ralf Loritz¹, Conrad Jackisch¹, Martijn Westhoff², Axel Kleidon³,
5 Theresa Blume⁴, Sibylle Hassler¹, Hubert, H. Savenije⁵

6 1) Karlsruhe Institute of Technology (KIT), 2) Vrije Universiteit Amsterdam, The Netherlands, 3),
7 Max Planck Institute for Bio-Geo-Chemistry, Jena 4), GFZ German Research Centre for
8 Geosciences 5) Delft Technical University.

9 Abstract: The present study corroborates that the free energy state of soil water offers a new
10 perspective on storage dynamics and similarity of hydrological systems that cannot be
11 inferred from the usual comparison of soil moisture observations or groundwater levels. We
12 show that the unsaturated zone of any hydrological system is characterized by a system-
13 specific balance of storage and release. This storage equilibrium, which is jointly controlled
14 by the soil physical and topographical system characteristics, reflects the thermodynamic
15 equilibrium state of minimum free energy the system approaches when relaxing from external
16 disturbances. Rainfall or radiation frequently forces parts of the system out of this storage
17 equilibrium, storage dynamics can hence be visualized as sequences of deviations from and
18 relaxations back to equilibrium. This perspective reveals that storage dynamics operates in
19 two distinctly different energetic regimes, where either capillarity dominates over gravity or
20 vice versa. As these regimes are associated either with a storage deficit or a storage excess,
21 relaxation requires either recharge or release. This implies that the terms ‘wet’ and ‘dry’
22 should be used with respect to the equilibrium storage as meaningful reference point. We
23 show furthermore that the free energy state of the soil water stock, the storage equilibrium
24 which separates the two dynamic regimes, as well as the degree of non-linearity within those
25 regimes depend on the joint controls of catchment topography and the physical properties of
26 the soils. We express these joint controls in form of a new characteristic function of the
27 unsaturated zone we call the ‘energy state function’. By comparing the energy state functions
28 of different systems we demonstrate their distinct sensitivity to topography and soil water
29 characteristics and their usefulness for inter-comparing storage dynamics among those
30 systems. This ultimately reveals that storage dynamics at the system level may operate by far
31 more linearly than suggested by the retention function of the soils.



32 **1 INTRODUCTION**

33 **1.1 Motivation**

34 ‘The whole is greater than the sum of the parts’ - Savenije and Hrachowitz (2017) grounded
35 their recent proposition that catchments function similarly to meta-organisms on this famous
36 quote of Aristotle. Their blue print essentially suggests that catchments evolve towards a
37 configuration which balances water storage and release in an optimal manner. This idea is
38 largely motivated by their more specific finding of an optimum rooting depth (Gao et al.,
39 2014), which likely balances the advantage of vegetation to endure droughts of increasing
40 return periods with the necessary energetic investment to grow their roots to deeper and
41 deeper water stocks. The present study revisits the idea that hydrological systems balance
42 storage and release suggested by Savenije and Hrachowitz (2017), using a thermodynamic
43 perspective on soil water dynamics (Zehe et al., 2013). More specifically we propose that this
44 balance connects to the thermodynamic equilibrium state the system approaches when
45 relaxing from external disturbance driven by either rainfall or radiative forcing.

46 **1.2 Thermodynamic reasoning in hydrology**

47 Thermodynamic reasoning in earth sciences may be traced back to the early work of Leopold
48 and Langbein (1962) on the role of entropy in the evolution of landforms. Thermodynamics
49 gained however substantial attention in catchment hydrology since the work of Kleidon and
50 Schymanski (2008). Kleidon and Schymanski (2008) discussed the opportunity of using
51 thermodynamic optimality such as maximum entropy production (MEP, Paltridge, 1979) or
52 maximum power (Lotka, 1922a; Lotka, 1922b) for uncalibrated hydrological predictions. This
53 vision has motivated several efforts to predict the catchment water balance using MEP either
54 to determine parameters controlling root water uptake (Porada et al., 2011) or to optimize the
55 splitting of rainfall into recharge and (surface) runoff (Westhoff and Zehe, 2013; Zehe et al.,
56 2013). Other studies investigated the role of connected flow networks such as river networks
57 or rill systems and suggested that they increase the power in coupled water and sediment
58 fluxes (Howard, 1990; Favis-Mortlock et al., 2000; Paik and Kumar, 2010; Kleidon et al.,
59 2013). This is because these networks minimize local dissipative losses for instance in the
60 river network (Rinaldo et al., 1996) or in subsurface preferential flow paths (Zehe et al., 2010;
61 Hergarten et al., 2014). Recent studies employed thermodynamic optimality approaches to
62 predict partitioning of net short wave radiation into long wave outgoing radiation and
63 turbulent fluxes of latent and sensible heat (Kleidon et al., 2014; Renner et al., 2016), to



64 derive the Budyko curve (Wang et al., 2015; Westhoff et al., 2014; Westhoff et al., 2016), to
65 explain root water uptake (Hildebrandt et al., 2016) or to infer parameters controlling salt
66 water intrusion into estuaries (Zhang and Savenije, 2018).

67

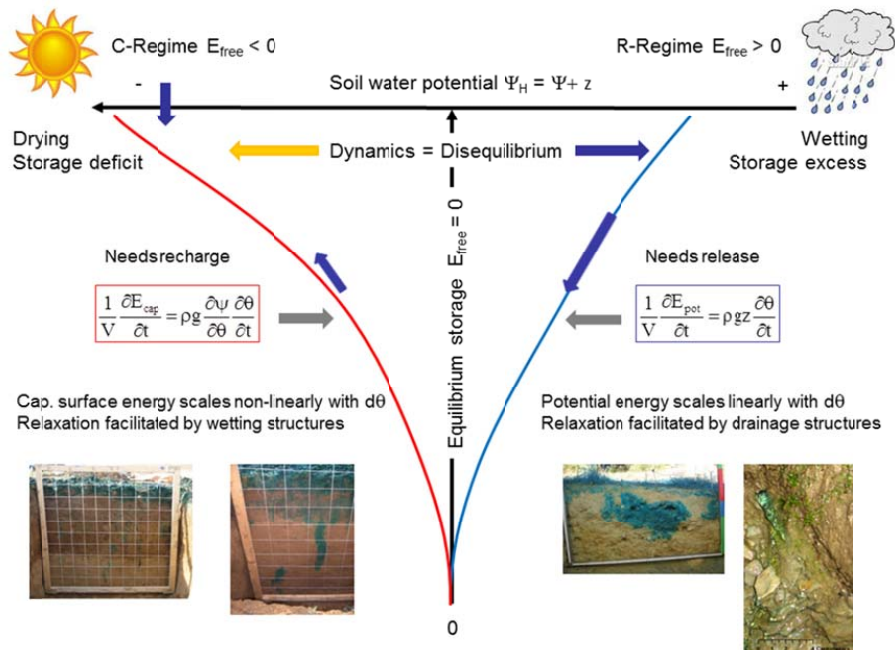
68 While the potential of thermodynamic optimality for uncalibrated predictions is an exciting
69 issue, a thermodynamic perspective alone has a lot to offer to hydrological sciences. For
70 instance it can be used to explain hydrological similarity based on a thermodynamically
71 meaningful combination of catchment characteristics (Zehe et al., 2014; Seibert et al., 2017;
72 Loritz et al., 2018). Or it motivated the effort to develop models of intermediate complexity,
73 for instance based on the idea of a representative elementary watershed REW (Reggiani et al.,
74 1998a; Reggiani et al., 1998b; Reggiani et al., 1999; Reggiani et al., 2000; Reggiani and
75 Schellekens, 2003; Lee et al., 2005; Zhang et al., 2005; Tian et al., 2006; Lee et al., 2007;
76 Sivapalan, 2018). Closely related to this, thermodynamic reasoning has also been used to
77 upscale effective soil water characteristics (Zehe et al., 2006; de Rooij, 2009) partly for
78 closure of the REW approach. In this study we propose that thermodynamic reasoning offers a
79 radically new, energy based perspective on storage dynamics and similarity of hydrological
80 systems that cannot be inferred from the usual comparison of soil moisture observations or
81 groundwater levels.

82 **1.3 The 'energy perspective' on soil water storage**

83 In line with Savenije and Hrachowitz (2017) we propose that the unsaturated zone of any
84 hydrological system is characterized by a system-specific balance of storage and release. This
85 balance, which is jointly controlled by the soil physical and topographical characteristics,
86 relates to the thermodynamic equilibrium of the system, as it corresponds to a state of
87 minimum free energy of the soil water stock. In the absence of an external rainfall or radiative
88 forcing, the system will thus naturally relax back to this storage equilibrium and remain in this
89 state. Hydrological systems are however not isolated, which implies that they are frequently
90 forced out of their equilibrium either by rainfall or by radiation (Fig. 1). Here we show that
91 storage dynamics can be visualized as deviations of the free energy state of soil water from
92 this storage equilibrium. This reveals that these deviations and subsequent relaxations operate
93 in two distinctly different energetic regimes, which are associated with either with a storage
94 excess or a storage deficit relative to the equilibrium state. Radiation driven evaporation and
95 transpiration force the system out of its equilibrium into a state range where capillarity
96 dominates against gravity, or in energetic terms, capillary surface energy of soil water is in



97 absolute terms larger than its potential energy. We thus call this the “C-regime”, because
 98 capillary surface energy differences act as dominant driver of soil water dynamics. The
 99 system is in a state of a storage deficit as it needs to recharge water for relaxation, but the
 100 necessary recharge amount is determined by the energetic distance to equilibrium. In contrary,
 101 rainfall driven recharge pushes the system into a state range where gravity dominates against
 102 capillarity, or in energetic terms, capillary surface energy of soil water is in absolute terms
 103 smaller than its potential energy. We call this the ‘P-regime’ because soil water dynamics is
 104 predominantly controlled by potential energy differences. The system is in a state of storage
 105 excess. It needs to release water to relax back to equilibrium and the necessary amount is
 106 determined by its energetic distance from equilibrium.



107
 108 Figure 1 (from Zehe et al (2013), modified): Thermodynamic equilibrium in a soil profile above the
 109 ground water surface as state of zero total hydraulic potential. Drying pulls the system into the C-
 110 regime by increasing absolute values of negative capillary surface energy. Wetting pushes the system
 111 into the P-regime by increasing potential energy of soil water. The expression for capillary surface
 112 energy and potential energy of soil water and their dynamic change with the soil water content are
 113 derived in section 2.1. The brilliant blue image highlight that relaxation back to equilibrium is in both
 114 regimes facilitated by different types of preferential pathways, those shown in the left favor recharge
 115 those shown to the right favor release.

116



117 As further detailed in the discussion section, relaxation back to equilibrium and thus
118 dissipation of free energy is in both regimes accelerated by preferential pathways, which
119 either favor recharge of the dry soil matrix to deplete the storage deficit or release of water to
120 deplete the storage excess (Zehe et al. 2013).

121 **1.4 Objectives**

122 In the following we show that the free energy state of the soil water stock, the distribution of
123 equilibrium storage values in a system, as well as the degree of non-linearity within the
124 aforementioned regimes depend on the joint controls of catchment topography, the
125 groundwater surface and the physical properties of the soils. These joint controls can be
126 expressed in form of a new characteristic function, which relates free energy of soil water to
127 a) the relative saturation of the soil, b) the corresponding matric/soil water potential and c) the
128 topographic elevation above groundwater. As this function characterizes the possible range of
129 “energy states” of soil water stored in the system, we call it the vadose zone “energy state
130 function”. By comparing the energy state functions of different systems we demonstrate their
131 distinct sensitivity to topography and soil water characteristics. We show furthermore that soil
132 water dynamics at single plots or within an entire hydrological system can, in case of a slowly
133 varying groundwater table, be nicely visualized as deviations from the storage equilibrium
134 either into the P- or the C-regime and subsequent relaxation due recharge or release of water.
135 This offers new opportunities for inter-comparing storage dynamics among different systems,
136 to explain differences in the corresponding of runoff generation and to which degree the point
137 scale non-linearity of soil physical properties affects storage dynamics at the system level.

138 **2 THEORY**

139 In the following we express the drivers of soil water dynamics, the soil water or matric
140 potential and the gravity potential, in energetic terms and then derive the energy state
141 function. As the latter depends on the elevation above the groundwater surface and the
142 retention function of the soils, we present those energy state functions for observed soil water
143 retentions from different landscapes to illustrate its sensitivity to those factors.

144 **2.1 Free energy of the soil water**

145 Latest since the work of Iwata et al. (1995) it is known that energetic state of water stored in
146 unsaturated soil depends on its potential energy and the surface energy at the air-water
147 interface. We may hence express the change in Helmholtz free energy (J) of the amount of



148 water stored in a small control volume dV (m^3) based on the changes in its potential energy
149 and of the surface energy at the air-water-interface (Iwata et al., 1995) ¹:

150

$$151 \quad dE_{\text{free}} = gz_{\text{GW}}dM + \sigma dA \quad (\text{Eq. 1})$$

152

153 Where g (ms^{-2}) is the acceleration of the earth and dM (kg) denotes a change in the stored
154 water mass, z_{GW} (m) is the depth above the groundwater surface, σ (N/m) is the surface
155 tension of water and dA (m^2) the change in the area of the water air interface. When
156 expressing dM as product of the water density ρ (kgm^{-3}) and a change in the volume of the
157 water phase dV_{θ} (m^3) we obtain:

158

$$159 \quad \begin{aligned} \text{a) } dE_{\text{free}} &= \rho gz_{\text{GW}}dV_{\theta} + \sigma dA \Leftrightarrow \\ \text{b) } \frac{\partial E_{\text{free}}}{\partial V_{\theta}} &= \rho gz_{\text{GW}} + \sigma \frac{\partial A}{\partial V_{\theta}} \quad \text{Eq. (2)} \end{aligned}$$

160

161 Particularly Eq. 2b) highlights that a change in the volume of the water phase implies, on one
162 hand a change in its potential energy. On the other hand it leads to changes in the surface
163 energy, as the air-water-interface and its curvature change with changing soil water content as
164 well. In the next step we employ the definition of the soil water potential ψ (m) for a spherical
165 air-water-interface with curvature radius r (m) to eliminate the surface tension in Eq. 2:

166

$$167 \quad \psi = \frac{2\sigma}{\rho gr} \Leftrightarrow \sigma = \frac{r}{2} \rho g \psi(\theta) \quad \text{Eq. (3)}$$

168

169 This yields the following expressions to characterise the change in free energy as function of a
170 changing volume of the water phase:

171

$$172 \quad \begin{aligned} \text{a) } dE_{\text{free}} &= \rho gz_{\text{GW}}dV_{\theta} + \frac{r}{2} \rho g \psi(\theta) \frac{\partial A}{\partial V_{\theta}} dV_{\theta} \Leftrightarrow \\ \text{b) } \frac{\partial E_{\text{free}}}{\partial V_{\theta}} &= \rho gz_{\text{GW}} + \frac{r}{2} \rho g \psi(\theta) \frac{\partial A}{\partial V_{\theta}} \quad \text{Eq. (4)} \end{aligned}$$

173

¹ Note that we assume isothermal conditions and neglect volumetric changes of the pore space.



174 Note the change rate in surface area of a sphere with changing radius and the related change
 175 rate in volume are as follows:

176

$$\begin{aligned}
 & \text{a) } \frac{\partial A_{\theta}}{\partial r} = 8\pi r \vee \frac{\partial V_{\theta}}{\partial r} = 4\pi r^2 \Leftrightarrow \\
 & \text{b) } \frac{\partial A_{\theta}}{\partial V_{\theta}} = \frac{\partial A_{\theta}}{\partial r} \frac{\partial r}{\partial V_{\theta}} = \frac{2}{r} \quad \text{Eq. (5)}
 \end{aligned}$$

178

179 By inserting Eq. 5 b) into Eq. 4 we obtain our final expressions describing the change in free
 180 energy of soil water as function of a change in the stored water in the control volume:

181

$$\begin{aligned}
 & \text{a) } dE_{\text{free}} = \rho g z_{\text{GW}} dV_{\theta} + \rho g \psi(\theta) dV_{\theta} \Leftrightarrow \\
 & \text{b) } \frac{\partial E_{\text{free}}}{\partial V_{\theta}} = \rho g z_{\text{GW}} + \rho g \psi(\theta) \quad \text{Eq. (6)}
 \end{aligned}$$

183

184 In the following we denote the first term on the right hand side as potential energy and the
 185 second one as capillary surface energy of soil water. Note that the latter is negative as the soil
 186 water potential is as a suction head negative as well. The stored water amount in a small
 187 control volume is equal to the product of the volume V and of the soil water content θ ($\text{m}^3 \text{m}^{-3}$).
 188 Hence, a change in the stored water amount relates either to a dynamic change in the soil
 189 water content, while the control volume size remains constant, or an increasing size of the
 190 control volume when moving up scale at a constant time:

191

$$\begin{aligned}
 & V_{\theta} = \theta V \Leftrightarrow \\
 & dV_{\theta} = V d\theta + \theta dV \quad \text{Eq. (7)}
 \end{aligned}$$

193

194 Local dynamic changes in the soil water stock, usually described by the Darcy-Richards
 195 equation, change thus the local free energy state of the soil water as well:

196

$$\frac{1}{V} \frac{\partial E_{\text{free}}}{\partial t} = \rho g z_{\text{GW}} \frac{\partial \theta}{\partial t} + \rho g \frac{\partial \psi(\theta)}{\partial \theta} \frac{\partial \theta}{\partial t} \quad \text{Eq. (8)}$$

198

199 This opens opportunities to analyze and visualize soil water dynamics through changes of the
 200 corresponding free energy state, as further detailed below. From equations 6 and 7 we can



201 also derive the free energy of soil water stored in a finite control volume at a constant time.
202 This is in fact equal to the integral of the product of the total hydraulic potential, $\psi + z_{GW}$, and
203 the soil water content over the volume of interest (de Rooij, 2009; Zehe et al., 2013):

$$205 \quad E_{\text{free}} = E_{\text{cap}} + E_{\text{pot}} = \int \rho g (\psi(\theta) + z_{\text{GW}}) \theta dV \quad \text{Eq. (9)}$$

206
207 The two drivers in Darcy's law, the soil water potential and the gravity potential, reflect thus
208 in fact the weight-specific capillary surface energy and the weight specific potential energy of
209 soil water. Note that the potential energy of soil water grows with increasing storage while
210 capillary surface energy shrinks as the soil water potential declines with increasing wetness.
211 From equation 8 it becomes furthermore clear that capillary surface energy is in accordance
212 with the non-linear shape of the soil water retention curve the main source of non-linearity in
213 soil water dynamics and in its free energy state, because it scales with the slope of the
214 retention curve. The energy perspective reveals, however, nicely that potential energy of soil
215 water is at a given elevation above the groundwater surface a linear function of the soil water
216 content. This already indicates that dominance of the one or the other energy form is
217 important for the question whether a system behaves in a linear or non-linear fashion.

218 **2.2 Equilibrium storage and energy state at a depth to groundwater**

219 The state of minimum free energy is reached when $\partial E_{\text{free}} / \partial V_{\theta} = 0$. Due to Eq. (6) this is the
220 case when the system is in hydraulic equilibrium, where Ψ equals the negative of z_{GW}
221 everywhere in the subsurface:

$$223 \quad \begin{aligned} \rho g (\psi + z_{\text{GW}}) \theta = 0 &\Leftrightarrow \\ \psi = -z_{\text{GW}} &\quad (\text{Eq. 10}) \end{aligned}$$

224
225 The soil hydraulic equilibrium corresponds hence to a state where the absolute value of the
226 free energy of soil water is minimal, because the specific potential energy of soil water equals
227 its specific capillary surface energy density at any point in the subsurface. Note that this
228 means equivalently that the system is in a state of perfect mixing, and thus maximum mixing
229 entropy, due to the absent gradient in hydraulic potential (Kondepudi and Prigogine, 1998;
230 Iwata et al., 1995). The equilibrium storage at any point in the system can be inferred from the



231 water retention curves of the soils in a straightforward manner by substituting the soil water
 232 potential by the depth to the groundwater water surface (e.g. Porada et al., 2011):

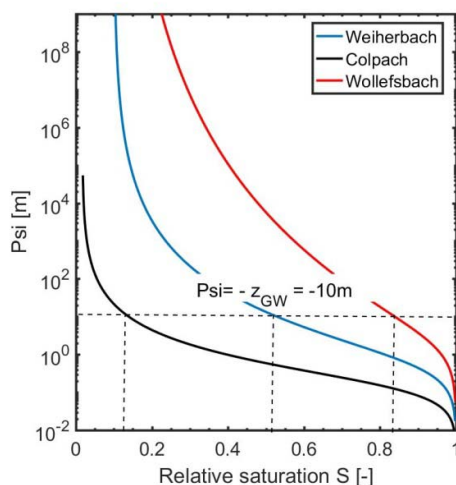
233

$$234 \quad S_{eq} \equiv \frac{\theta}{\theta_s} |(\psi = -z_{GW}) \text{ Eq. (11)}$$

235

236 Where θ_s (m^3m^{-3}) is the saturated soil water content and S (-) is the relative saturation. This is
 237 illustrated in figure 2 for the retention curves of three distinctly different soils, assuming
 238 arbitrarily a depth to groundwater of $z_{GW} = 10$ m. The equilibrium saturation of the clay rich
 239 soil in the Marl geological setting of the Wollefsbach catchment is with $S_{eq} = 0.82$ rather large,
 240 while the young silty soil located in the Colpach has a rather small saturation at equilibrium of
 241 $S_{eq} = 0.13$. The loess soil from the Weiherbach is with $S_{eq} = 0.53$ in between these extremes.
 242 Note that two of those soils are located in our respective study areas Colpach and Wollefsbach
 243 (compare section 3). We added the Weiherbach soil to complete the spectrum of possible
 244 endmembers.

245



246

247 Figure 2: Soil water retention curves as function of relative saturation determined as explained in
 248 section 3.3. The dashed black lines mark the relative saturation at hydraulic equilibrium, assuming
 249 arbitrarily a depth to groundwater of $z_{GW} = 10$ m. The Wollefsbach and the Colpach are further
 250 characterised in section 3.

251



252 Note that although these values are very different in magnitude, they represent the respective
253 equilibrium storage states, which these systems at this elevation will naturally approach when
254 relaxing from external disturbances. And it is exactly those equilibrium storages which
255 separate the aforementioned state ranges where the system is either in a storage deficit or in a
256 storage excess. This becomes obvious when plotting the specific free energy per unit volume
257 e_{free} (m) of the soil water stock as function of the relative saturation for these soils (Fig. 3).
258 The latter can be obtained by deriving Eq. 9 with respect to V and normalising it with ρg :

259

$$260 \quad e_{\text{free}} \equiv \frac{1}{\rho g} \frac{\partial E_{\text{free}}}{\partial V} \equiv (\psi(\theta) + z_{\text{GW}}) \cdot \theta = f\left(\frac{\theta}{\theta_s} \mid z_{\text{GW}} = \text{const}\right) \text{ Eq. (12)}$$

261

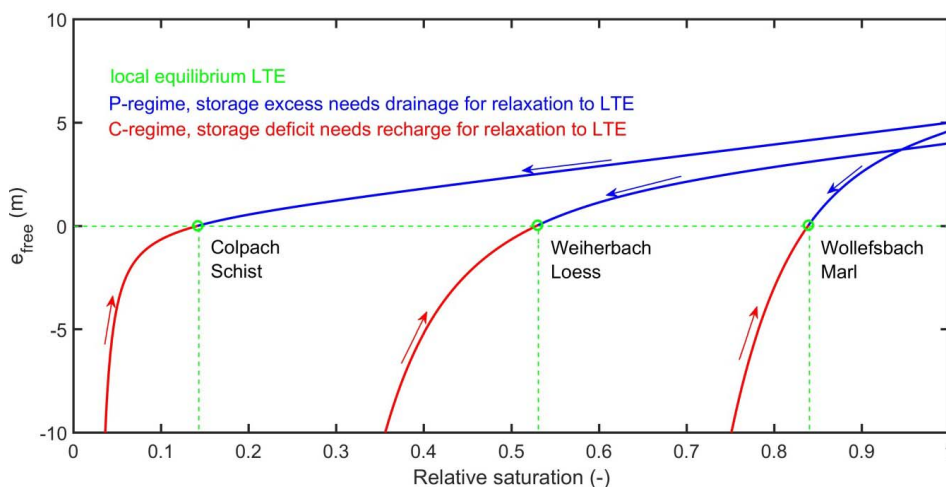
262 Note e_{free} is, as being defined as free energy per unit volume, equal to the product of total
263 hydraulic potential and the soil water content. It thus differs from the total hydraulic potential,
264 which is the free energy per wetted control volume.

265

266 The horizontal green line in Figure 3 marks the local equilibrium state where the absolute
267 value of the specific free energy at this particular elevation is zero. The vertical lines indicate
268 the corresponding equilibrium saturations at the x-axis (these correspond to those in figure 2).
269 In case of a constant depth to groundwater, these equilibrium storages separate the ranges of
270 soil saturation belonging to the P-regime (in blue) from those that belong to the C-regime (in
271 red), respectively. In the P-regime e_{free} is positive as e_{pot} is larger than the absolute value of
272 e_{cap} . Storage dynamics are hence dominated by potential energy differences and thus gravity.
273 In the P-regime, the system is locally in a state of storage excess because it has with respect to
274 its equilibrium too much potential energy. One might thus expect that the system needs - in
275 absence of an external rainfall forcing - to release water from this elevation to relax back to
276 equilibrium. Note that the necessary amount of water that needs to be released is determined
277 by the overshoot of free energy above zero. In the C-regime specific free energy gets negative
278 as capillary surface energy becomes larger than the potential energy. Storage dynamics are
279 dominated by local capillary controls. The system needs to recharge water to deplete the “free
280 energy deficit” below zero, and the necessary amount depends on the free energy deficit
281 below zero.

282

283



284

285 Figure 3: Weight specific free energy state of the soil water stock, as defined in Eq. (12), plotted
286 against the relative saturation of the three different soils, assuming a depth to groundwater of 10m.
287 The green lines mark the local equilibrium state where the absolute value of the specific free energy is
288 zero and the corresponding equilibrium saturations. Free energy in the P-regime and C-regimes are
289 plotted in solid blue and red respectively, the arrows indicate the way back to equilibrium.

290

291 Note that we assume the local soil volume to be in capillary contact with the groundwater
292 surface (see section 5.2 for further discussion). It is clear that in case of a dynamic
293 groundwater table, the equilibrium storage and the energy state function at a distinct depth
294 will change. The same holds in case of a constant depth to groundwater, when moving
295 vertically through the unsaturated zone, as explained in the next section.

296 2.3 The energy state function of the unsaturated zone

297 From equation 12 and the graphs in Fig. 3 it is only a small step to derive the energy state
298 function for the unsaturated zone of any hydrological system, with a fixed groundwater level
299 or where the groundwater level is known as function of time. Specific free energy of the soil
300 water stock depends jointly on the retention curve of a point in the unsaturated zone and its
301 elevation above the groundwater surface. This implies that the energy state curves in a system
302 of interest change also with the range of elevations above groundwater. In the following we
303 illustrate this for the idealized case of a landscape with a single soil and a well-defined single
304 retention function.

305



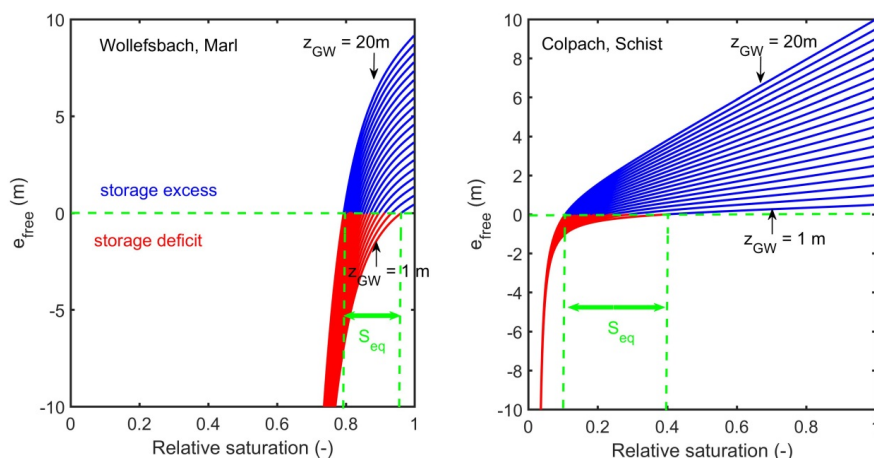
306 Common ways to characterize the topographic distribution in a catchment are either by means
 307 of the hypsometric integral, taking the catchment outlet as reference, or by means of the
 308 height over nearest drainage (HAND, Renno et al., 2008; Nobre et al., 2011), taking the
 309 closest stream as reference. Here we extend the idea of HAND from the land surface to the
 310 entire unsaturated zone of a catchment, using optionally the water level in the next channel as
 311 a proxy for the depth of the groundwater surface and its changes. We may hence characterize
 312 the ‘family’ of energy state curves describing free energy of soil water at different elevations
 313 above groundwater if we know a) the retention functions of the soils and b) the range of
 314 HAND, $R(z_{GW})$, in the system of interest, as follows:

315

$$316 \quad e_{\text{free}}(\text{soil}, z_{\text{GW}}) = (\psi_{\text{soiltype}}(\theta) + z_{\text{GW}}) \cdot \theta = f\left(\frac{\theta}{\theta_s}, z_{\text{GW}}\right), z_{\text{GW}} \in R(z_{\text{GW}}) \text{ Eq. (13)}$$

317

318 The energy state function consists thus of a family of curves, characterizing how depth to
 319 groundwater and soil physical characteristics jointly control the free energy state of soil water
 320 as function of the relative saturation. Please note that all points with the same soil water
 321 retention curve and the same elevation above groundwater are represented by the same energy
 322 state curve.



323

324 Figure 4: Energy state function, characterizing the specific free energy state of soil water as function
 325 or relative saturation, soil water retention and depth to groundwater. Each of the 20 curves represents a
 326 distinct depth above the groundwater surface for a discrete range of 1m to 20 m. The vertical green
 327 lines mark the range of the equilibrium saturations S_{eq} at the different elevations.



328 Figure 4 gives an impression of how the energy state functions would look like, in case the
329 soils of the Colpach and the Wollefsbach were distributed along an elevation range above
330 groundwater of $R=[1\text{m}, 20\text{m}]$. Note that we assume that the soil water retention function in
331 figure 1 is valid everywhere in this hypothetical landscape. Figure 4 depicts that the individual
332 energy state curves of the family become generally steeper and the P-range becomes generally
333 wider with an increasing depth to groundwater. This reflects a) the increasing importance of
334 potential energy and b) the decreasing equilibrium saturation with increasing depth to
335 groundwater. The shape of the individual curves and the equilibrium storage are for both
336 hypothetical systems distinctly different. Given those strongly different shapes of the energy
337 state functions one might expect the two systems to exhibit strongly different storage
338 dynamics. We further elaborate on these differences in section 3, when introducing the energy
339 state functions of our study areas.

340 **3 APPLICATION**

341 The energy state function introduced in the last section defines the space of possible energy
342 states of the soil water stock, a thermodynamic state space of the unsaturated zone at the level
343 system so to say. Due to the intermittent atmospheric forcing and the exchange of the soil
344 water with atmosphere, groundwater body and river, parts of the system are frequently pushed
345 and pulled out of its equilibrium into states of the either P or the C regime. It appears thus
346 straightforward to visualize these storage dynamics, either observed or modeled, as pseudo²
347 oscillations of the corresponding free energy state in the respective energy state functions.
348 This will teach us a) which part of the state space is actually visited by the system, and b)
349 whether the system predominantly operates in one of these regimes or within both them. In
350 the following we briefly characterize the study areas and the dataset we use for this purpose.

351 **3.1 Study areas and their energy state functions**

352 The Colpach and the Wollefsbach catchments belong to the Attert experimental basin (Pfister
353 et al., 2002; Pfister et al., 2017), and are distinctly different with respects to soils, topography,
354 geology and landuse (Fig. 5a). Both catchments have been extensively characterized in
355 previous studies with respect to their physiographic characteristics, dominant runoff
356 generation mechanisms and available data (Wrede et al., 2015; Martinez-Carreras et al., 2015;
357 Loritz et al., 2017; Angermann et al., 2017). Hence, we focus here exclusively on those

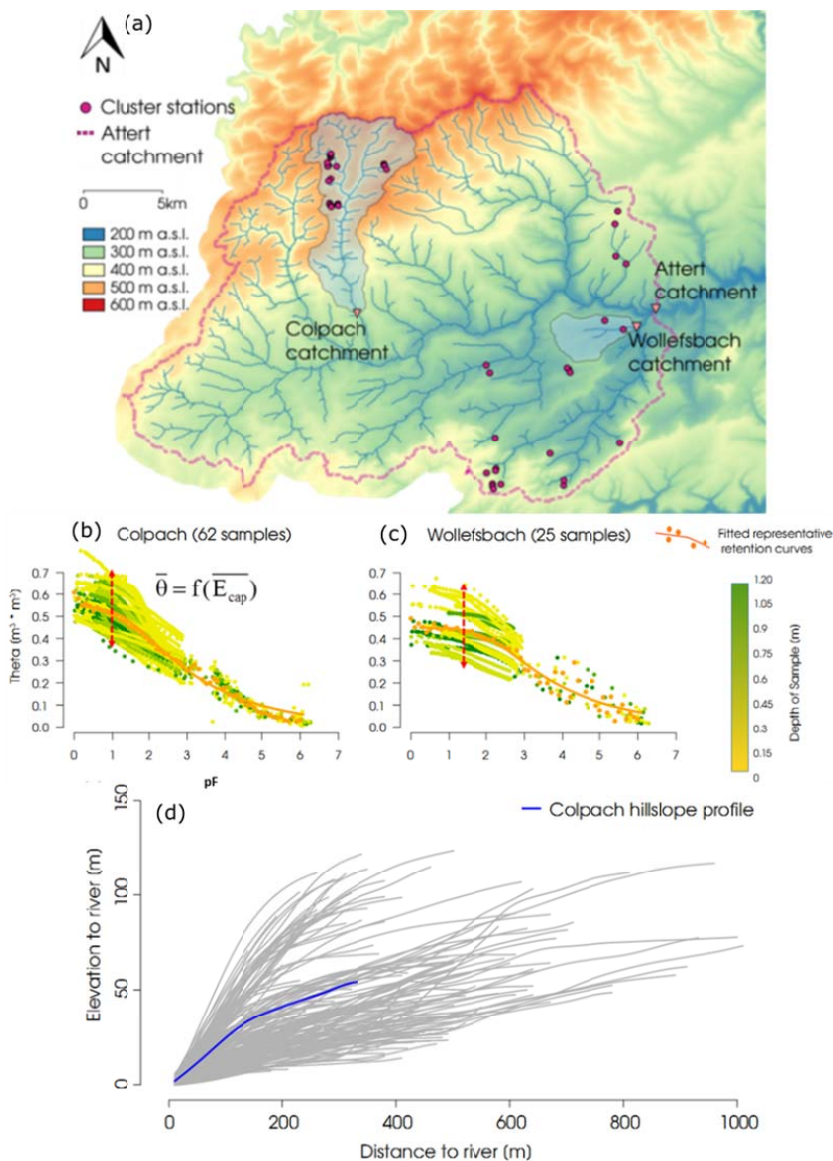
² We use the term pseudo here, as these are in fact deviations into different directions and relaxations to LTE. These are no oscillations in a strictly mechanical sense.



358 system characteristics which determine their respective energy state functions. The Colpach
359 has an elevation range from 265 to 512 m. Soils are young silty haplic Cambisols that formed
360 on schistose periglacial deposits. Despite of their high silt content they are characterized by a
361 high permeability and high porosity (Jackisch et al., 2017), because the fine silt aggregates
362 embed a fast draining network of coarse inter-aggregate pores. In contrary, the Wollefsbach
363 has a much more gentle topography from 245 to 306 to m.a.s.l. Soils in this marl geological
364 setting range from sandy loams to thick clay lenses. Soil water retention was in both
365 catchments analyzed by Jackisch (2015) using a set of 62 undisturbed soil cores from the
366 Colpach and 28 undisturbed soil cores from the Wollefsbach.

367 Here we do not use these point relations but a representative, macroscale soil water retention
368 function to derive the energy state function of our study areas. These were derived by
369 Jackisch (2015) from the raw data of all experiments as follows. He pooled the matching pairs
370 of soil water content and matric potential of all experiments in a landscape into a single
371 sample (Fig. 5 b and c), which hence characterizes the spreading of saturations at a given
372 tension that occurred in these systems. By averaging the soil water content at each matric
373 potential/tension-level he obtained an aggregated data set characterizing the relation between
374 the average soil water content that is stored at a given soil water potential/tension. The
375 representative retention curves were finally optioned by fitting the van Genuchten-Mualem
376 relation to the aggregate data (Jackisch, 2015). Note that this relation cannot be observed at a
377 single site, it is a macroscale relation which characterizes the average behavior in the entire
378 system. More importantly this approach preserves the relation between the average soil water
379 content and the specific capillary surface energy and it has been shown to perform superior
380 during a process based simulation of the water balance in both areas, which represented the
381 system by a single representative hillslope (Loritz et al, 2017). The topography of these
382 representative hillslopes corresponds in both cases to the distribution of HAND, which
383 implies that the distribution function of potential energy along the flow path to the stream is
384 preserved (Fig. 5d). By combining these representative hillslopes with the representative
385 retention functions we finally obtained the energy state functions of the Colpach (Fig. 6 a) and
386 the Wollefsbach (Fig. 6 b).

387

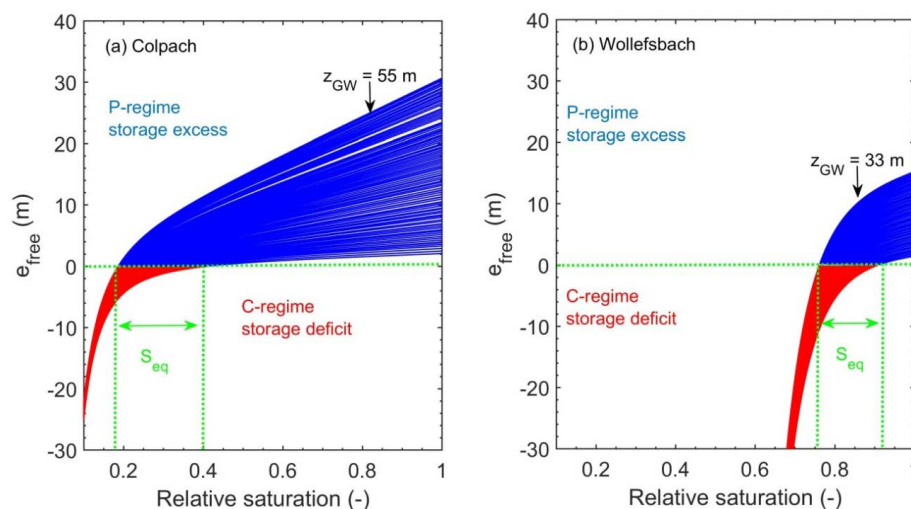


388

389 Figure 5: Map of the Atert basin with the Colpach and Wollefsbach catchments (Panel a, taken from
 390 Loritz et al. 2017). The red dots mark the cluster sites of the CAOS research unit, which collect
 391 besides the standard hydro-meteorological data, soil moisture and the soil water potential. Panel b and
 392 c present the data from the soil water content as function of tension observed in a large set of multistep
 393 outflow experiments and the representative retention curves obtained by energy conservative
 394 averaging. Panel d show the distribution of HAND for the hillslope in the Colpach catchment and of
 395 the effective hillslope Loritz et al. (2017) derived for his model study, the corresponding distribution
 396 in the Wollefsbach is not shown, as it is due to the homogeneous topography rather straightforward.



397 Note that the larger elevation range in the Colpach causes a clear dominance of the P-Regime
 398 over a wide range of saturation. More importantly figure 6a reveals that for relative
 399 saturations larger than 0.4 free energy is a multilinear function of relative saturation. This
 400 means that the specific free energy is at each geopotential level a linear function of relative
 401 saturation, but the slope of the energy state curves does increase with increasing distance to
 402 groundwater. In contrary the Wollefsbach is clearly a non-linear system within the entire
 403 range of elevations, with clearly much smaller maximum free energy but with a huge potential
 404 for strongly negative free energy when soils dry out. Consistently, we find the ranges of
 405 equilibrium saturation in the systems to be rather different, between 0.95 and 0.78 in the
 406 Wollefsbach and between 0.4 down to 0.18 in the Colpach.



407
 408 Figure 6: Energy state functions of the Colpach (a) and the Wollefsbach (b) derived from the range of
 409 HAND and the representative retention functions in figure 4. The horizontal green line mark the
 410 equilibrium of zero free energy, the vertical green lines mark the corresponding ranges of equilibrium
 411 saturations.

412 3.2 Available storage observations

413 We use data from a distributed network of 45 sensor clusters spread across the entire Attert
 414 experimental basin (Figure 4) collected within the hydrological year 2013/14. These clusters
 415 measure, among other variables, soil moisture and soil water potentials within three replicated
 416 profiles in 0.1, 0.3 and 0.5 m depths using Decagon 5TE capacitive soil moisture sensors. As



417 direct observations of groundwater levels are rare and only available close to riparian zone we
418 use the height over the next stream to estimate z_{GW} .

419 **4 RESULTS**

420 **4.1 Soil moisture and its free energy state at two distinct cluster sites**

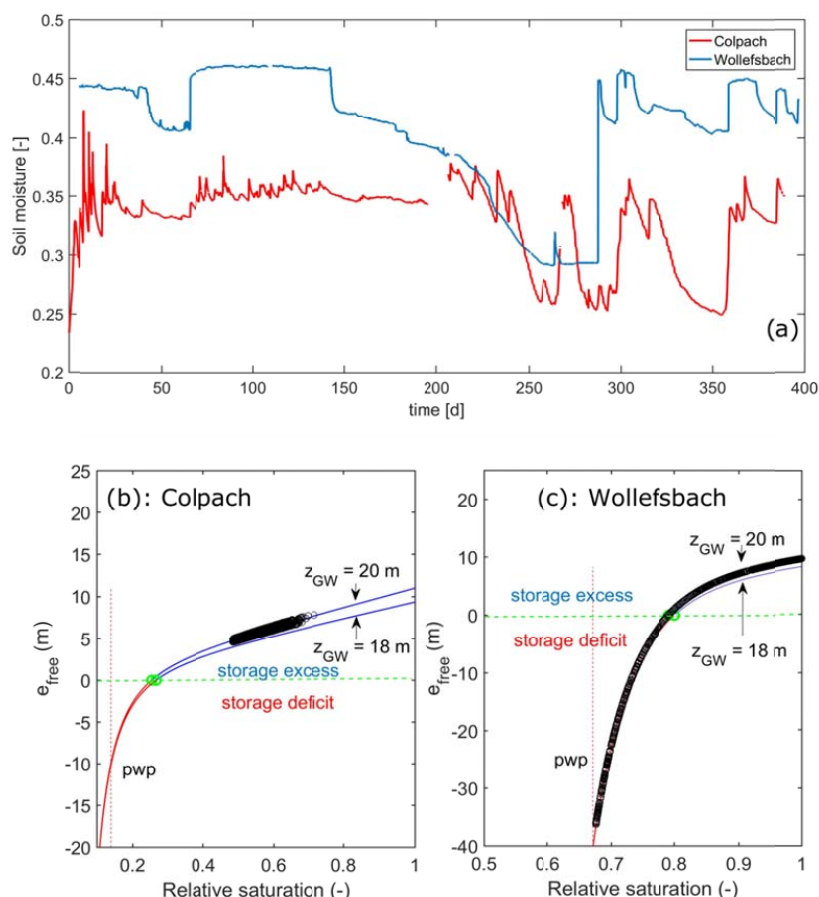
421 In a first step we inter-compare the free energy states of the soil moisture stock (Fig. 7) which
422 was observed at two arbitrarily selected sites in the respective study catchments. Both sites are
423 located 20 m above their respective streams. The soil water content in the clay rich top soil of
424 the Wollefsbach site is in the winter and fall period rather uniform and on average $0.12 \text{ m}^3 \text{ m}^{-3}$
425 larger than in the Colpach (Fig. 7a). While the soil water content at the Colpach site appears
426 much more variable in these periods. Both sites dry out considerably during the summer
427 period and start to recharge with the beginning of the fall.

428

429 Figure 7 b and c provide the corresponding free energy states of both soil water time series as
430 function of the soil saturation. Observations are shown as black circles and the related
431 theoretical energy state curves, calculated after Eq. 12. The first thing to note is that the
432 observed free energy states for both sites scatter nicely around the theoretical curves. More
433 interestingly one can see that the spreading of the free energy state of the soil water stock is at
434 both sites distinctly different, while the ranges of the corresponding soil water contents are
435 comparable. The free energy state of soil water at the Colpach site is during the entire
436 hydrological year in the P-regime and hence subject to an overshoot in potential energy (Fig.
437 7b). The site operates in the linear range of the energy state curve and fluctuates around an
438 average energy height of 6.0 m, which corresponds to an average energy density of $5.9 \cdot 10^4$
439 Jm^{-3} . While the observations spread across a total range of 3 m ($2.9 \cdot 10^4 \text{ Jm}^{-3}$) their standard
440 deviation is 0.31 m ($3.0 \cdot 10^3 \text{ Jm}^{-3}$). The coefficient of variation of the free energy state is
441 hence with 0.05 rather small. In contrary the specific free energy of the soil water stock in the
442 Wollefsbach spreads across a much wider range of almost 50m, which corresponds to $4.9 \cdot 10^5$
443 Jm^{-3} (Fig. 7c). The average specific free energy is with 4.8 m ($4.7 \cdot 10^4 \text{ Jm}^{-3}$) clearly smaller as
444 at the Colpach site, while the coefficient of variation is with 1.3 much larger. Most
445 importantly the system operates qualitatively differently as it switches to the C regime and



446 thus a strong storage deficit during dry spells in the summer period. Please note that the free
 447 energy declines to the value corresponding to the permanent wilting point pwp^3 .
 448



449
 450 Figure 7: Top soil water content observed at cluster sites in the Colpach and the Wollefsbach
 451 catchment (panel a) and the corresponding free energy states in their respective energy state curves
 452 (panel b and c). The black circles mark the observations. The vertical dashed line marks the permanent
 453 wilting point, which is due to the definition of the total free energy in Eq. 6 not simply equal to a total
 454 hydraulic potential of -133 m. Panels b and c show additionally the energy state curve for $z_{GW} = 18$ m,
 455 to highlight that an error in the estimated depth to groundwater implies a substantial mismatch
 456 between observations and the theoretically predicted curve.
 457

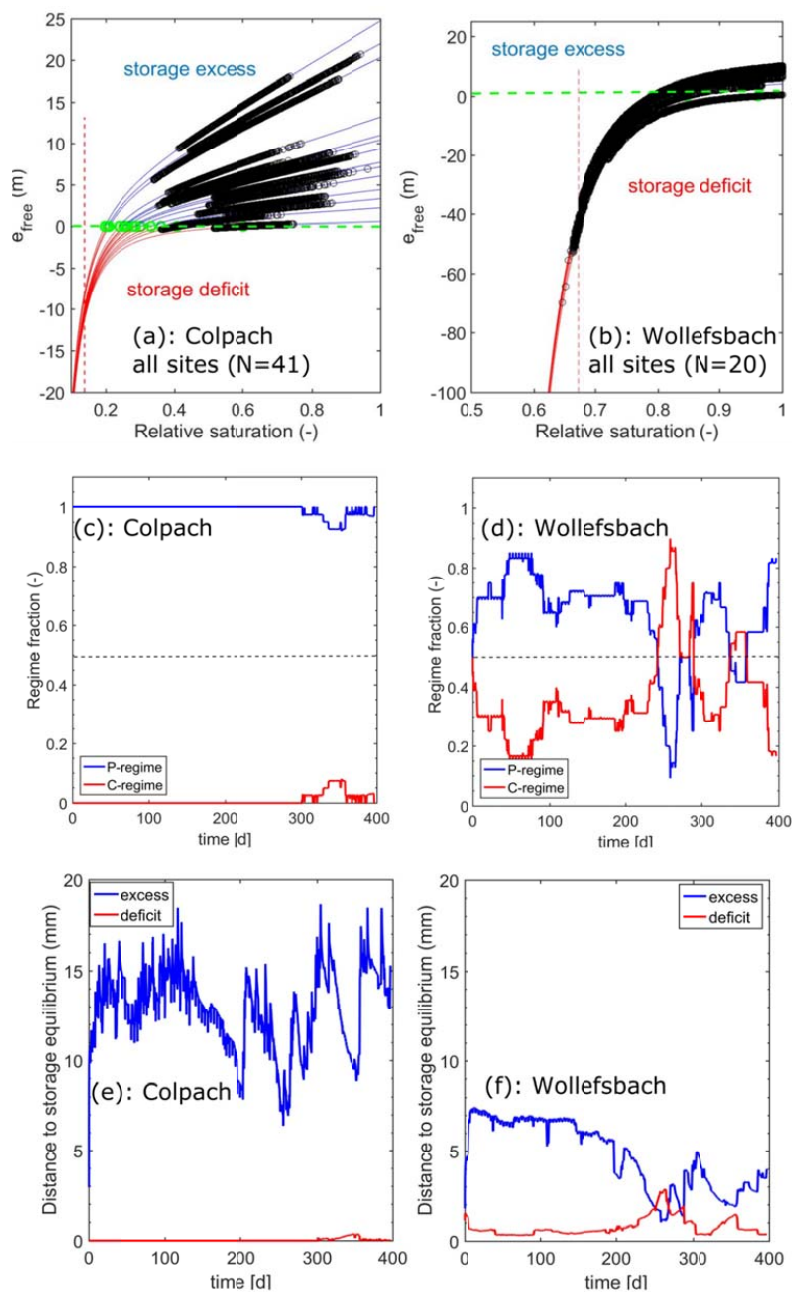
³ As specific free energy is according to Eq. (12) the product of the total soil hydraulic potential and the soil water content, its value at the pwp does not simply correspond to -133m.



458 We hence state that the free energy state of the soil water stock reveals a distinctly different
459 dynamic behavior of both sites, which cannot be derived from the inter comparison of the
460 corresponding soil water moisture time series. The Colpach site is characterized by permanent
461 storage excess, though the corresponding soil water content is nearly always smaller than in
462 the Wollefsbach. Free energy of the soil water stock is a linear function of relative saturation.
463 In contrary, the Wollefsbach shows a strongly non-linear behavior at this site and it switches
464 to a storage deficit when the soil saturation drops below 0.78, which corresponds to a soil
465 water content of $0.374 \text{ m}^3 \text{ m}^{-3}$ (Fig. 7a). We thus wonder whether the term wet and dry should
466 therefore be used with respect to the equilibrium storage as meaningful reference point. Last
467 but not least the theoretical energy level curves derived for a distance to groundwater of $z_{\text{GW}} =$
468 18 m do not fit the corresponding observations but show a clear negative bias (Figure 7b,c).
469 An error in the estimated depth to groundwater implies thus a substantial mismatch between
470 the observations and the theoretically predicted energy curve. This implies that energy levels
471 will also change with changing groundwater surface, as further detailed in the discussion.

472 **4.2 Soil moisture and its free energy state within the entire observation** 473 **domain**

474 Figure 8 presents the free energy states of the top soil moisture which was observed at all
475 cluster sites in the Colpach (panel a, $N = 41$) and the Wollefsbach (panel b, $N = 20$). The
476 respective heights above the channel range from 1 to 45 m in the Colpach and from 1 to 22m
477 in the Wollefsbach. Generally, the observed free energy states scatter again nicely around the
478 energy state curves of the corresponding z_{GW} . The Colpach operates, except for the sites
479 located at the smallest distances to groundwater ($z_{\text{GW}} = 1$ and 4m), in the linear range of the P-
480 regime, indicating that soil moisture dynamics is dominated by potential energy differences.
481 Free energy of the soil water stock is hence a multi linear function of saturation. The total set
482 of observations in the Colpach generally spread across a wide range of relative saturations,
483 and the corresponding “amplitudes” of the free energy deviations are clearly larger as at the
484 single site shown in Figure 7 b. This is because sensor clusters with the same estimated height
485 above groundwater were pooled into the same subsample regardless of their separating
486 distance. For instance at $z_{\text{GW}} = 1$ m the subsample consisted of 1 cluster with three replicate
487 soil moisture profiles, at $z_{\text{GW}} = 17$ we had for instance 3 sensor clusters and thus in total 9 soil
488 moisture profiles. The partly large spreading of the observations may hence be explained by a
489 combination of local scale heterogeneity and large scale differences in the drivers of soil
490 water dynamics such as rainfall or local characteristics of forest vegetation.



491

492 Figure 8: Free energy of all observations in the Colpach (a) and Wollefsbach (b) plotted in their
 493 corresponding energy state function (note the different scales). The black circles mark the
 494 observations. The horizontal green lines mark the equilibrium of zero free energy. Panel c and d show
 495 which fractions of the data set was in the P or in the C regime as function of time. Panel e and f show
 496 the averaged distance to storage equilibrium for the sites in a storage deficit and a storage excess.



497 Despite of the large spreading between 80 -100% of the Colpach sites operated permanently
498 in the P-Regime (Fig. 8c). During the wet season it is 100% of the sites, between day 300 and
499 400, the profiles at the lowest distance to groundwater switch into the C-regime and thus a
500 storage deficit. Fig. 8 e shows the average distance to storage equilibrium in mm as function
501 of time. Sites with storage excess are on average 13 mm above their equilibrium, the
502 minimum is 6 mm. The average top soil storage deficit (we show this as positive value) is the
503 entire observation period rather small. This suggests that the top soil sites in the Colpach may
504 the during entire observation period release water either to the subsoil or in down slope
505 direction.

506

507 In the Wollefsbach we find, consistently with figure 7b, a drop of free energy into the C-
508 regime during the dry summer period. Storage dynamics in the entire system works, in
509 accordance with the shape of the energy level function, in a strongly non-linear manner. Note
510 that a few values drop even below the permanent wilting point. This can either be explained
511 by the fact that local vegetation is more efficient in root water uptake as sun flowers (the
512 model crop to define the permanent wilting point), or by measurement errors. In contrary to
513 the Colpach, the fractions of profiles which operate in the C-regime or in the P-regime are
514 much more variable in time (Fig. 8d). On average 30% of the profiles operate in a storage
515 deficit during the entire observation period, the minimum is 15% and the C-regime fraction
516 peaks at 90% at day 250. Consistently, we find that the storage excess in the Wollefsbach is
517 on average 3 mm, while the average storage deficit is much more prominent; it even exceeds
518 the storage excess during the summer period (Fig. 8e). These differences are consistent with
519 the strongly different runoff generation behavior of both systems, as further detailed in the
520 discussion.

521 **5 DISCUSSION AND CONCLUSIONS**

522 The presented results provide strong evidence that a thermodynamic perspective on soil water
523 storage provides holistic information for judging and inter-comparing the storage state and
524 storage dynamics of hydrological systems, which cannot be inferred from soil moisture
525 observations alone. In the following we reflect the general idea of using free energy as state
526 measure, discuss its promises as well as its limiting assumptions. We then move on to the
527 more specific differences in the storage dynamics in both our study systems. And we close by
528 reflecting on the seeming paradox between the known local non-linearity of soil physical



529 characteristics and the frequent argumentation that hydrological systems often behave much
530 more linearly.

531 **5.1 Free energy and the energy level function – options and limitations**

532 Our results clearly show that free energy as function of relative soil saturation holds the key to
533 defining a meaningful state space of a hydrological system, regardless of its spatial extent.

534 This space of possible energy states consists of a family of energy state curves, where each of
535 those characterizes how free energy density evolves at a distinct elevation above ground
536 water, depending on the triad of the matric potential, gravity potential (i.e. depth to
537 groundwater) and soil water content. The free energy state of soil water reflects in fact the
538 balance between its capillary surface energy and geo potential energy densities and we
539 showed that this balance determines:

- 540 • Whether a system is at given elevation above groundwater locally in its equilibrium
541 storage state ($e_{\text{free}} = 0$), in a state of a storage deficit ($e_{\text{free}} < 0$) or in state of a storage
542 excess ($e_{\text{free}} > 0$);
- 543 • The regime of storage dynamics. Soil water dynamics in the C-regime ($e_{\text{free}} < 0$) are
544 dominated by capillarity i.e. the local, non-linear soil physical driver, which means the
545 system needs recharge to relax to its equilibrium. Or it is in the P-regime ($e_{\text{free}} > 0$)
546 dominated by potential energy, i.e. the non-local linear gravitational control, which
547 means the system needs to release water to relax to local equilibrium.

548 The energy level function turned out to be useful for inter-comparing distributed soil moisture
549 observations among different hydrological landscapes, as it shows the trajectory of single sites
550 or of the complete set of observations in its state space. This teaches us which part of the state
551 space is actually ‘visited’ by the system during the course of time, whether the system
552 operates predominantly in a single regime, whether it switches between both regimes and how
553 much water needs to be released or recharged locally for relaxing back to local equilibrium
554 and how often it actually is at equilibrium or if it never gets there. Note that the usual
555 comparison of soil water contents alone did not yield this information. On the contrary from
556 this we would conclude that the site in the Wollefsbach is, due to the higher soil water
557 content, always ‘wetter’ than the corresponding site in the Colpach. The free energy state
558 reveals, however, the exact opposite, we have a storage excess at Colpach site for the entire
559 year while the Wollefsbach site is in summer in a storage deficit. We thus propose that the



560 term wet and dry should only be used with respect to the equilibrium storage as meaningful
561 reference point.

562

563 The apparent strong sensitivity of the free energy state of the soil water stock to the estimated
564 depth to groundwater offers on the one hand new opportunities for data based learning and an
565 improved design of measurement campaigns, but it also determines the limit of the proposed
566 approach. With respect to the first aspect, we could show that an error of 2 m in the assumed
567 depth to groundwater lead to a clear deviation of the observed free energy states from the
568 theoretical energy level curve. This offers either the opportunity to estimate depth to
569 groundwater from joint observations of soil moisture and matric potential, in case the local
570 retention function is known. This can be done by minimizing the residuals between the
571 observation and the theoretical curve as function of depth to groundwater. Or it allows for the
572 derivation of a retention function based on the joint observations of soil moisture, matric
573 potential and depth to groundwater. Here, we need again to minimize the residuals between
574 the observation and the theoretical curve but this time as function of the parameters of the soil
575 water retention curve. Due this strong sensitivity it is furthermore important to stratify soil
576 moisture observations both according to the installed depth of the probe and according to the
577 elevation of the site above groundwater, or the height over the next stream. The former is
578 important because the soil above overlaying the sensor acts as a low pass filter. The latter is
579 important because depth to groundwater determines the equilibrium storage the site will
580 approach when relaxing from external forcing.

581

582 Despite of all these opportunities for learning, the sensitivity of free energy to the depth to
583 groundwater implies that the site of the system is still in hydraulic contact with the aquifer.
584 This key assumption is certainly violated if the soil gets so dry that the water phase becomes
585 immobile while the air phase becomes the mobile phase. And it might get violated if depth to
586 groundwater becomes too large. Last but not least the groundwater surface may change either
587 seasonally, or in some systems more rapidly, and this changes $z_{GW}(t)$ in the energy level
588 function and the storage equilibrium. We nevertheless conclude that it is worth to collect joint
589 data sets either of the triple of soil moisture, matric potential and the retention function at
590 distributed locations (as we did in the CAOS research unit as explained in (Zehe et al. 2014))
591 or even preferable on the quadruple of soil moisture, matric potential, retention function and



592 depth to groundwater. Soil moisture observations alone appear not very informative about the
593 system state.

594 **5.2 Storage dynamics in different landscapes – local versus non local** 595 **controls**

596 More specifically we found that soil water dynamics in the Colpach and the Wollefsbach
597 exhibit a substantial difference. The observations clearly revealed that the Colpach operates
598 the entire hydrological year in a state of storage excess due to an overshoot in potential
599 energy. Soil water dynamics is mainly driven by potential energy, which means that the linear
600 and non-local gravitational control is dominant. Most interestingly we found that the free
601 energy state of the soil operated in the linear range of the P-regime, which implies that the
602 storage dynamics is (multi) linear. This means that the specific free energy is at each
603 geopotential level a linear function of relative saturation, but the slope of the energy state
604 curves does increase with increasing distance to groundwater

605

606 We found furthermore that the annual variation of the averaged free energy of the soil water
607 stock was rather small. Zehe et al. (2013) found a similar, almost steady state behavior, for the
608 free energy of the soil water stock in the Mallalcahuello catchment in Chile, which also
609 operated in the P-regime the entire year. Note that both landscapes are characterized by a
610 pronounced topography, by well drained highly porous soils (Blume et al., 2008a; Blume et
611 al., 2008b; Blume et al., 2009) and that both are predominantly forested. And in both
612 landscape subsurface storm flow is the dominant runoff generation process, as gravity is the
613 dominant control of soil water dynamics.

614 On the contrary the Wollefsbach was characterized by a seasonal change between both
615 regimes: operation in the P-regime during the wet season and a drop to a strong storage deficit
616 during the dry summer period when operation in the C-regime. Free energy was at all sites is
617 a clearly non-linear function of the relative saturation. Interestingly we found the same
618 seasonality for the Weiherbach catchment in Germany, a dominance of potential energy
619 during the wet season and a strong dominance of capillary surface energy in summer (Zehe et
620 al 2013). Note that both landscapes are characterized by silty cohesive soils and a gentle
621 topography and both are used for agriculture. In both areas Hortonian overland flow would
622 play the dominant role, but this process is actually strongly reduced due to a large amount of
623 worm burrows acting as macropores. Both landscape are also controlled by tile drains, which
624 artificially controls depth to groundwater. In both areas the soil water dynamics is dominated



625 by capillarity during the summer period, which means that the local soil physical control
626 dominates also at the system level.

627

628 We thus suggest that similarity in those landscape attributes - which controls the energy level
629 function - implies qualitatively identical regimes of storage dynamics. We furthermore
630 wonder whether distinct differences in the energy state functions and more importantly of the
631 free energy states might help explaining differences in dominant runoff generation. In the
632 Colpach we found a clear storage excess in the top soil during the entire observation period,
633 while the in Wollefsbach the storage deficit exceeded storage excess in summer. This
634 difference might explain the strong difference in runoff generation. The Colpach is
635 characterized by a strong subsurface and base flow component while those are negligible in
636 the Wollefsbach.

637 **5.3 Free energy to assist hydrological predictions**

638 Although the scope of this study was on the usefulness of thermodynamics to diagnose and
639 explain different storage dynamics, we will add a short discussion on the predictive value of
640 this thermodynamic perspective. In this context it is important to recall that relaxation back to
641 equilibrium and thus dissipation of free energy is in both regimes accelerated by different
642 types of preferential pathways. Zehe et al (2013) distinguished wetting structure which favor
643 recharge of the dry soil matrix and deplete the storage deficit, from drainage structures which
644 favor water release and deplete the storage excess, because these affect free energy dynamics
645 of the soil water stock in largely different ways.

646

647 Drainage structures are preferential pathways that extend continuously through the
648 unsaturated zone either into the aquifer or to the riparian zone. Typical examples are
649 macropores that connect to subsurface pipe networks or tile drains (Zhang et al., 2006; Weiler
650 and McDonnell, 2007; Wienhofer et al., 2009; Wienhofer and Zehe, 2014; Nimmo, 2012,
651 2016; Gelbrecht et al., 2005; Klaus and Zehe, 2011; Klaus et al., 2014). They facilitate
652 bypassing and export of excess water and hence act similar to veins. They thereby accelerate
653 reduction of potential energy overshoot and thus relaxation from storage excess in the P-
654 regime. For systems which operate predominantly in the P-regime it is important to recall that
655 a steady state in the free energy balance does not imply a steady state of the water balance.
656 This has been shown by Zehe et al. (2013), by analyzing the free energy balance of rainfall
657 input, soil water storage and runoff. It does however imply a constant ratio between steady



658 storage and release, which can be calculated based on the upslope geo-potential and the
659 elevation where the system exports runoff to the stream (Zehe et al. 2013). For the
660 Mallacahuello catchment (Zehe et al. 2013) this turned out to be a reasonable estimate of the
661 average annual runoff coefficient. And a model structure which was, with respect to the
662 density of drainage structures, tuned to reproduce this energetic steady state was shown to
663 provide acceptable simulations of stream flow. It might thus be valuable to test whether we find
664 similar results for the Colpach.

665

666 The relaxation from the C-regime requires macropores which facilitate wetting and recharge
667 of the subsoil from dry initial conditions. This implies that these “wetting structures” do not
668 extend across the entire unsaturated zone, but end within the subsoil; typical examples are
669 worm burrows (Shipitalo and Edwards, 1996; Shipitalo and Butt, 1999; Zehe and Fluhler,
670 2001; Bastardie et al., 2003; Lindenmaier et al., 2005; Binet et al., 2006; van Schaik et al.,
671 2014) or shrinkage cracks (Vogel et al., 2005a; Vogel et al., 2005b; Zehe et al., 2007) or root
672 channels (Tobón-Marín et al., 2000; Abernethy and Rutherford, 2001; Gregory, 2006;
673 Johnson and Lehmann, 2006; Tietjen et al., 2009) or a network of conductive inter-aggregate
674 pores (Jackisch 2015; Jackisch et al. 2017). Wetting structures favor recharge as they allow a
675 bypassing of the dry and thus low conductive soil matrix and a subsequent wetting of the
676 subsoil across the macropore matrix interface (Beven and Germann, 2013; Jackisch and Zehe,
677 2018). They thereby accelerate depletion of gradients in soil water potential, reduce capillary
678 binding energy excess and accelerate relaxation from the storage deficit in the C-regime. In
679 those systems, which seasonally switch among both regimes, we may find a thermodynamic
680 optimal density of wetting structures that maximizes average dissipation of free energy during
681 recharge events. Zehe et al. (2013) showed that this optimum structure, which balances
682 recharge and surface runoff in an optimal way, allowed successful predictions of rainfall
683 runoff generation and the water balance in the Weiherbach catchment.

684

685 We thus conclude that idea of an optimum catchment configuration postulated by Savenije
686 and Hrachowitz (2017) is supported by our study. It might correspond to a thermodynamic
687 optimum and exist in those systems, which seasonally switch between the P and the C regime.
688 Note that such thermodynamic optimum maximizes dissipation of free energy during
689 relaxation back to equilibrium (Zehe et al. 2013), and this implies that the relaxation time
690 becomes minimal. Zehe et al. (2013) showed that such an optimum requires a preferential



691 flow network that balances wetting and drainage. Along similar lines the free energy state of
692 simulations might help in model assessment and evaluation. This approach is promising to
693 discriminate substantial model errors from insubstantial ones. A substantial error could be
694 defined for instance when the model and observation operate for longer periods in different
695 energetic regimes. Alternatively, one can explore how changes in system characteristics,
696 particularly macropores, affect how the system operates in the energetic phase space. And as
697 energy is an additive quantity one can derive an aggregated energy level function for the
698 entire system and test its feasibility of upscaling,

699 **5.4 Concluding remarks**

700 Overall we conclude that a thermodynamic perspective on hydrological systems provides
701 valuable insights which move beyond the exciting issue of using thermodynamic optimality
702 for uncalibrated predictions. Our most important finding is that the energy level function,
703 which can be seen as a straightforward generalization of the soil retention function, accounts
704 jointly for capillary and gravitational control on soil moisture dynamics. With this we bridge
705 the scale between local, non-linear soil physical controls and system level topographical
706 controls on storage dynamics. The beautiful outcome is that linear behavior at the system
707 level does not compromise the non-linearity of soil water characteristics. In contrary it may be
708 easily explained by the dominance of potential energy for catchments with pronounced
709 topography and during not too dry conditions. The option for linear behavior of hydrological
710 systems is inherent to Darcy's law for the unsaturated zone itself. The latter is likely the
711 reason why conceptual models, which usually do not account for soil physical characteristics,
712 work in some catchments very well and others don't. Based on the presented findings one
713 could speculate that conceptual models work well in system which are dominated by potential
714 energy, at least in the Attert experimental basin this statement is consistent with the study of
715 Wrede et al. (2015).

716

717 ACKNOWLEDGMENTS: This study contributes to and greatly benefited from the
718 "Catchments as Organized Systems" (CAOS) research unit. We sincerely thank the German
719 Research Foundation (DFG) for funding (FOR 1598, ZE 533/11-1, ZE 533/12-1). The authors
720 acknowledge support by Deutsche Forschungsgemeinschaft and the Open Access Publishing
721 Fund of Karlsruhe Institute of Technology (KIT). The service charges for this open access
722 publication have been covered by a Research Centre of the Helmholtz Association. The code
723 and the simulation projects underlying this study are freely available on request.

724 **6 REFERENCES**

- 725 Abernethy, B., and Rutherford, I. D.: The distribution and strength of riparian tree roots in
726 relation to riverbank reinforcement, *Hydrological Processes*, 15, 63-79, 2001.
- 727 Angermann, L., Jackisch, C., Allroggen, N., Sprenger, M., Zehe, E., Tronicke, J., Weiler, M.,
728 and Blume, T.: Form and function in hillslope hydrology: Characterization of
729 subsurface flow based on response observations, *Hydrology And Earth System
730 Sciences*, 21, 3727-3748, [10.5194/hess-21-3727-2017](https://doi.org/10.5194/hess-21-3727-2017), 2017.
- 731 Bastardie, F., Capowicz, Y., de Dreuzy, J.-R., and Cluzeau, D.: X-ray tomographic and
732 hydraulic characterization of burrowing by three earthworm species in repacked soil
733 cores, *Applied Soil Ecology*, 24, 3-16, 2003.
- 734 Beven, K., and Germann, P.: Macropores and water flow in soils revisited, *Water Resources
735 Research*, 49, 3071-3092, [10.1002/wrcr.20156](https://doi.org/10.1002/wrcr.20156), 2013.
- 736 Binet, F., Kersanté, A., Munier-Lamy, C., Le Bayon, R.-C., Belgy, M.-J., and Shipitalo, M. J.:
737 Lumbricid macrofauna alter atrazine mineralization and sorption in a silt loam soil, *Soil
738 Biology and Biochemistry*, 38, 1255-1263, 2006.
- 739 Blume, T., Zehe, E., and Bronstert, A.: Investigation of runoff generation in a pristine, poorly
740 gauged catchment in the chilean andes ii: Qualitative and quantitative use of tracers at
741 three spatial scales, *Hydrological Processes*, 22, 3676-3688, [10.1002/hyp.6970](https://doi.org/10.1002/hyp.6970), 2008a.
- 742 Blume, T., Zehe, E., Reusser, D. E., Iroume, A., and Bronstert, A.: Investigation of runoff
743 generation in a pristine, poorly gauged catchment in the chilean andes i: A multi-method
744 experimental study, *Hydrological Processes*, 22, 3661-3675, [10.1002/hyp.6971](https://doi.org/10.1002/hyp.6971), 2008b.
- 745 Blume, T., Zehe, E., and Bronstert, A.: Use of soil moisture dynamics and patterns at different
746 spatio-temporal scales for the investigation of subsurface flow processes, *Hydrology
747 And Earth System Sciences*, 13, 1215-1233, 2009.
- 748 de Rooij, G. H.: Averaging hydraulic head, pressure head, and gravitational head in
749 subsurface hydrology, and implications for averaged fluxes, and hydraulic conductivity,
750 *Hydrology And Earth System Sciences*, 13, 1123-1132, 2009.
- 751 Favis-Mortlock, D. T., Boardman, J., Parsons, A. J., and Lascelles, B.: Emergence and
752 erosion: A model for rill initiation and development, *Hydrological Processes*, 14, 2173-
753 2205, [10.1002/1099-1085\(20000815/30\)14:11/12<2173::aid-hyp61>3.0.co;2-6](https://doi.org/10.1002/1099-1085(20000815/30)14:11/12<2173::aid-hyp61>3.0.co;2-6), 2000.
- 754 Gao, H., Hrachowitz, M., Schymanski, S. J., Fenicia, F., Sriwongsitanon, N., and Savenije, H.
755 H. G.: Climate controls how ecosystems size the root zone storage capacity at
756 catchment scale, *Geophysical Research Letters*, 41, 7916-7923, [10.1002/2014gl061668](https://doi.org/10.1002/2014gl061668),
757 2014.
- 758 Gelbrecht, J., Lengsfeld, H., Pöthig, R., and Opitz, D.: Temporal and spatial variation of
759 phosphorus input, retention and loss in a small catchment of ne germany, *Journal of
760 Hydrology*, 304, 151-165, 2005.
- 761 Gregory, P. J.: Roots, rhizosphere and soil: The route to a better understanding of soil
762 science?, *European Journal of Soil Science*, 57, 2-12, 2006.
- 763 Hergarten, S., Winkler, G., and Birk, S.: Transferring the concept of minimum energy
764 dissipation from river networks to subsurface flow patterns, *Hydrology And Earth
765 System Sciences*, 18, 4277-4288, [10.5194/hess-18-4277-2014](https://doi.org/10.5194/hess-18-4277-2014), 2014.



- 766 Hildebrandt, A., Kleidon, A., and Bechmann, M.: A thermodynamic formulation of root water
767 uptake, *Hydrology And Earth System Sciences*, 20, 3441-3454, 10.5194/hess-20-3441-
768 2016, 2016.
- 769 Howard, A. D.: Theoretical model of optimal drainage networks, *Water Resour. Res.*, 26,
770 2107-2117, 1990.
- 771 Iwata, S., Tabuchi, T., and Warkentin, B. P.: Soil-water interactions, *Mechanisms and*
772 *applications*, M. Dekker, 1995.
- 773 Jackisch, C.: Linking structure and functioning of hydrological systems – How to achieve
774 necessary experimental and model complexity with adequate effort, PhD thesis, KIT
775 Karlsruhe Institute of Technology, <https://doi.org/10.5445/IR/1000051494>, 2015.
- 776 Jackisch, C., Angermann, L., Allroggen, N., Sprenger, M., Blume, T., Tronicke, J., and Zehe,
777 E.: Form and function in hillslope hydrology: In situ imaging and characterization of
778 flow-relevant structures, *Hydrology And Earth System Sciences*, 21, 3749-3775,
779 10.5194/hess-21-3749-2017, 2017.
- 780 Jackisch, C. and Zehe, E.: Ecohydrological particle model based on representative domains,
781 *Hydrol. Earth Syst. Sci. Discuss.*, <https://doi.org/10.5194/hess-2017-676>, accepted,
782 2018.
- 783 Johnson, M. S., and Lehmann, J.: Double-funneling of trees: Stemflow and root-induced
784 preferential flow, *Ecoscience*, 13, 324-333, 10.2980/i1195-6860-13-3-324.1, 2006.
- 785 Klaus, J., and Zehe, E.: A novel explicit approach to model bromide and pesticide transport in
786 connected soil structures, *Hydrology And Earth System Sciences*, 15, 2127-2144,
787 10.5194/hess-15-2127-2011, 2011.
- 788 Klaus, J., Zehe, E., Elsner, M., Palm, J., Schneider, D., Schroder, B., Steinbeiss, S., van
789 Schaik, L., and West, S.: Controls of event-based pesticide leaching in natural soils: A
790 systematic study based on replicated field scale irrigation experiments, *Journal Of*
791 *Hydrology*, 512, 528-539, 10.1016/j.jhydro1.2014.03.020, 2014.
- 792 Kleidon, A., and Schymanski, S.: Thermodynamics and optimality of the water budget on
793 land: A review, *Geophysical Research Letters*, 35, L20404 10.1029/2008gl035393,
794 2008.
- 795 Kleidon, A., Zehe, E., Ehret, U., and Scherer, U.: Thermodynamics, maximum power, and the
796 dynamics of preferential river flow structures at the continental scale, *Hydrology And*
797 *Earth System Sciences*, 17, 225-251, 10.5194/hess-17-225-2013, 2013.
- 798 Kleidon, A., Renner, M., and Porada, P.: Estimates of the climatological land surface energy
799 and water balance derived from maximum convective power, *Hydrology And Earth*
800 *System Sciences*, 18, 2201-2218, 10.5194/hess-18-2201-2014, 2014.
- 801 Kondepudi, D., and Prigogine, I.: *Modern thermodynamics: From heat engines to dissipative*
802 *structures*, John Wiley Chichester, U. K., 1998.
- 803 Lee, H., Sivapalan, M., and Zehe, E.: Representative elementary watershed (rew) approach, a
804 new blueprint for distributed hydrologic modelling at the catchment scale: The
805 development of closure relations, in: *Predicting ungauged streamflow in the mackenzie*
806 *river basin: Today's techniques and tomorrow's solutions*, edited by: Spence, C.,
807 Pomeroy, J., and Pietroniro, A., Canadian Water Resources Association (CWRA),
808 Ottawa, 165-218, 2005.



- 809 Lee, H., Zehe, E., and Sivapalan, M.: Predictions of rainfall-runoff response and soil moisture
810 dynamics in a microscale catchment using the crew model, *Hydrology And Earth*
811 *System Sciences*, 11, 819-849, 2007.
- 812 Leopold, L. B., and Langbein, W. L.: The concept of entropy in landscape evolution, *U.S.*
813 *Geol. Surv. Prof. Pap.*, 500-A, 1962.
- 814 Lindenmaier, F., Zehe, E., Dittfurth, A., and Ihringer, J.: Process identification at a slow-
815 moving landslide in the voralberg alps., *Hydrological Processes*, 19 1635-1651., 2005.
- 816 Loritz, R., Hassler, S. K., Jackisch, C., Allroggen, N., van Schaik, L., Wienhöfer, J., and
817 Zehe, E.: Picturing and modeling catchments by representative hillslopes, *Hydrol. Earth*
818 *Syst. Sci.*, 21, 1225-1249, [10.5194/hess-21-1225-2017](https://doi.org/10.5194/hess-21-1225-2017), 2017.
- 819 Loritz, R., Gupta, H., Jackisch, C., Westhoff, M., Kleidon, A., Ehret, U., and Zehe, E.: On the
820 dynamic nature of hydrological similarity, *Hydrol. Earth Syst. Sci. Discuss.*,
821 <https://doi.org/10.5194/hess-2017-739>, in review, 2018.
- 822 Lotka, A. J.: Contribution to the energetics of evolution, *Proc Natl Acad Sci USA*, 8, 147-151,
823 1922a.
- 824 Lotka, A. J.: Natural selection as a physical principle, *Proc Natl Acad Sci USA*, 8, 151-154,
825 1922b.
- 826 Martinez-Carreras, N., Wetzel, C. E., Frenress, J., Ector, L., McDonnell, J. J., Hoffmann, L.,
827 and Pfister, L.: Hydrological connectivity inferred from diatom transport through the
828 riparian-stream system, *Hydrology And Earth System Sciences*, 19, 3133-3151,
829 [10.5194/hess-19-3133-2015](https://doi.org/10.5194/hess-19-3133-2015), 2015.
- 830 Nimmo, J. R.: Preferential flow occurs in unsaturated conditions, *Hydrological Processes*, 26,
831 786-789, [10.1002/hyp.8380](https://doi.org/10.1002/hyp.8380), 2012.
- 832 Nimmo, J. R.: Quantitative framework for preferential flow initiation and partitioning, *Vadose*
833 *Zone Journal*, 15, [10.2136/vzj2015.05.0079](https://doi.org/10.2136/vzj2015.05.0079), 2016.
- 834 Nobre, A. D., Cuartas, L. A., Hodnett, M., Renno, C. D., Rodrigues, G., Silveira, A.,
835 Waterloo, M., and Saleska, S.: Height above the nearest drainage - a hydrologically
836 relevant new terrain model, *Journal Of Hydrology*, 404, 13-29,
837 [10.1016/j.jhydrol.2011.03.051](https://doi.org/10.1016/j.jhydrol.2011.03.051), 2011.
- 838 Paik, K., and Kumar, P.: Optimality approaches to describe characteristic fluvial patterns on
839 landscapes, *Philos. Trans. R. Soc. B-Biol. Sci.*, 365, 1387-1395,
840 [10.1098/rstb.2009.0303](https://doi.org/10.1098/rstb.2009.0303), 2010.
- 841 Paltridge, G. W.: Climate and thermodynamic systems of maximum dissipation, *Nature*, 279,
842 630-631, [10.1038/279630a0](https://doi.org/10.1038/279630a0), 1979.
- 843 Pfister, L., Iffly, J., and Hoffmann, L.: Use of regionalized stormflow coefficients with a view
844 to hydroclimatological hazard mapping, *Hydrological Sciences Journal-Journal Des*
845 *Sciences Hydrologiques*, 47, 479-491, 2002.
- 846 Pfister, L., Martinez-Carreras, N., Hissler, C., Klaus, J., Carrer, G. E., Stewart, M. K., and
847 McDonnell, J. J.: Bedrock geology controls on catchment storage, mixing, and release:
848 A comparative analysis of 16 nested catchments, *Hydrological Processes*, 31, 1828-
849 1845, [10.1002/hyp.11134](https://doi.org/10.1002/hyp.11134), 2017.



- 850 Porada, P., Kleidon, A., and Schymanski, S. J.: Entropy production of soil hydrological
851 processes and its maximisation, *Earth Syst. Dynam.*, 2, 179-190, 10.5194/esd-2-179-
852 2011, 2011.
- 853 Reggiani, P., Hassanizadeh, S. M., and Sivapalan, M.: A unifying framework for watershed
854 thermodynamics: Balance equations for mass, momentum, energy and entropy, and the
855 second law of thermodynamics, *Advances in Water Resources*, 22, 367-398, 1998a.
- 856 Reggiani, P., Sivapalan, M., and Hassanizadeh, S. M.: A unifying framework for watershed
857 thermodynamics: Balance equations for mass, momentum, energy and entropy, and the
858 second law of thermodynamics, *Advances In Water Resources*, 22, 367-398, 1998b.
- 859 Reggiani, P., Hassanizadeh, S. M., Sivapalan, M., and Gray, W. G.: A unifying framework for
860 watershed thermodynamics: Constitutive relationships, *Advances In Water Resources*,
861 23, 15-39, 1999.
- 862 Reggiani, P., Sivapalan, M., and Hassanizadeh, S. M.: Conservation equations governing
863 hillslope responses: Exploring the physical basis of water balance, *Water Resources*
864 *Research*, 36, 1845-1863, 2000.
- 865 Reggiani, P., and Schellekens, J.: Modelling of hydrological responses: The representative
866 elementary watershed approach as an alternative blueprint for watershed modelling,
867 *Hydrological Processes*, 17, 3785-3789, 2003.
- 868 Renner, M., Hassler, S. K., Blume, T., Weiler, M., Hildebrandt, A., Guderle, M., Schymanski,
869 S. J., and Kleidon, A.: Dominant controls of transpiration along a hillslope transect
870 inferred from ecohydrological measurements and thermodynamic limits, *Hydrology*
871 *And Earth System Sciences*, 20, 2063-2083, 10.5194/hess-20-2063-2016, 2016.
- 872 Renno, C. D., Nobre, A. D., Cuartas, L. A., Soares, J. V., Hodnett, M. G., Tomasella, J., and
873 Waterloo, M. J.: Hand, a new terrain descriptor using srtm-dem: Mapping terra-firme
874 rainforest environments in amazonia, *Remote Sensing of Environment*, 112, 3469-3481,
875 10.1016/j.rse.2008.03.018, 2008.
- 876 Rinaldo, A., Maritan, A., Colaiori, F., Flammini, A., and Rigon, R.: Thermodynamics of
877 fractal networks, *Physical Review Letters*, 76, 3364-3367, 1996.
- 878 Savenije, H. H. G., and Hrachowitz, M.: Hess opinions "catchments as meta-organisms - a
879 new blueprint for hydrological modelling", *Hydrology And Earth System Sciences*, 21,
880 1107-1116, 10.5194/hess-21-1107-2017, 2017.
- 881 Seibert, S. P., Jackisch, C., Ehret, U., Pfister, L., and Zehe, E.: Unravelling abiotic and biotic
882 controls on the seasonal water balance using data-driven dimensionless diagnostics,
883 *Hydrology And Earth System Sciences*, 21, 2817-2841, 10.5194/hess-21-2817-2017,
884 2017.
- 885 Shipitalo, M. J., and Edwards, W. M.: Effects of initial water content on macropore/matrix
886 flow and transport of surface-applied chemicals, *Journal of Environmental Quality*, 25,
887 662-670, 1996.
- 888 Shipitalo, M. J., and Butt, K. R.: Occupancy and geometrical properties of lumbricus terrestris
889 I. Burrows affecting infiltration, *Pedobiologia*, 43, 782-794, 1999.
- 890 Sivapalan, M.: From engineering hydrology to earth system science: Milestones in the
891 transformation of hydrologic science, *Hydrology And Earth System Sciences*, 22, 1665-
892 1693, 10.5194/hess-22-1665-2018, 2018.



- 893 Tian, F., Hu, H., Lei, Z., and Sivapalan, M.: Extension of the representative elementary
894 watershed approach for cold regions via explicit treatment of energy related processes,
895 *Hydrology And Earth System Sciences*, 10, 619-644, 2006.
- 896 Tietjen, B., Zehe, E., and Jeltsch, F.: Simulating plant water availability in dry lands under
897 climate change: A generic model of two soil layers, *Water Resources Research*, 45,
898 W01418
899 10.1029/2007wr006589, 2009.
- 900 Tobón-Marin, C., Bouten, W., and Dekker, S. C.: Forest floor water dynamics and root water
901 uptake in four forest ecosystems in northwest amazonia, *Journal of Hydrology*, 237,
902 169-183, 2000.
- 903 van Schaik, L., Palm, J., Klaus, J., Zehe, E., and Schroeder, B.: Linking spatial earthworm
904 distribution to macropore numbers and hydrological effectiveness, *Ecohydrology*, 7,
905 401-408, 10.1002/eco.1358, 2014.
- 906 Vogel, H.-J., H., H., and Roth, K.: Studies of crack dynamics in clay soil i: Experimental
907 methods, results and morphological quantification., *Geoderma*, 125, 203-211, 2005a.
- 908 Vogel, H.-J., Hoffmann, H., Leopold, A., and Roth, K.: Studies of crack dynamics in clay soil
909 ii: A physically-based model for crack formation *Geoderma*, 125, 213 - 225, 2005b.
- 910 Wang, D. B., Zhao, J. S., Tang, Y., and Sivapalan, M.: A thermodynamic interpretation of
911 budyko and I'vovich formulations of annual water balance: Proportionality hypothesis
912 and maximum entropy production, *Water Resources Research*, 51, 3007-3016,
913 10.1002/2014wr016857, 2015.
- 914 Weiler, M., and McDonnell, J. J.: Conceptualizing lateral preferential flow and flow networks
915 and simulating the effects on gauged and ungauged hillslopes, *Water Resources
916 Research*, 43, W03403
917 10.1029/2006wr004867, 2007.
- 918 Westhoff, M., Zehe, E., Archambeau, P., and Dewals, B.: Does the budyko curve reflect a
919 maximum-power state of hydrological systems? A backward analysis, *Hydrology And
920 Earth System Sciences*, 20, 479-486, 10.5194/hess-20-479-2016, 2016.
- 921 Westhoff, M. C., and Zehe, E.: Maximum entropy production: Can it be used to constrain
922 conceptual hydrological models?, *Hydrology And Earth System Sciences*, 17, 3141-
923 3157, 10.5194/hess-17-3141-2013, 2013.
- 924 Westhoff, M. C., Zehe, E., and Schymanski, S. J.: Importance of temporal variability for
925 hydrological predictions based on the maximum entropy production principle,
926 *Geophysical Research Letters*, 41, 67-73, 10.1002/2013gl058533, 2014.
- 927 Wienhofer, J., Germer, K., Lindenmaier, F., Farber, A., and Zehe, E.: Applied tracers for the
928 observation of subsurface stormflow at the hillslope scale, *Hydrology And Earth System
929 Sciences*, 13, 1145-1161, 2009.
- 930 Wienhofer, J., and Zehe, E.: Predicting subsurface stormflow response of a forested hillslope -
931 the role of connected flow paths, *Hydrology And Earth System Sciences*, 18, 121-138,
932 10.5194/hess-18-121-2014, 2014.
- 933 Wrede, S., Fenicia, F., Martinez-Carreras, N., Juilleret, J., Hissler, C., Krein, A., Savenije, H.
934 H. G., Uhlenbrook, S., Kavetski, D., and Pfister, L.: Towards more systematic



- 935 perceptual model development: A case study using 3 luxembourgish catchments,
936 Hydrological Processes, 29, 2731-2750, 10.1002/hyp.10393, 2015.
- 937 Zehe, E., and Fluhler, H.: Slope scale variation of flow patterns in soil profiles, Journal of
938 Hydrology, 247, 116-132, 2001.
- 939 Zehe, E., Lee, H., and Sivapalan, M.: Dynamical process upscaling for deriving catchment
940 scale state variables and constitutive relations for meso-scale process models,
941 Hydrology And Earth System Sciences, 10, 981-996, 2006.
- 942 Zehe, E., Elsenbeer, H., Lindenmaier, F., Schulz, K., and Blöschl, G.: Patterns of
943 predictability in hydrological threshold systems, Water resources research, 43,
944 doi.10.1029/2006WR005589, 2007.
- 945 Zehe, E., Blume, T., and Blöschl, G.: The principle of 'maximum energy dissipation': A novel
946 thermodynamic perspective on rapid water flow in connected soil structures, Philos.
947 Trans. R. Soc. B-Biol. Sci., 365, 1377-1386, 10.1098/rstb.2009.0308, 2010.
- 948 Zehe, E., Ehret, U., Blume, T., Kleidon, A., Scherer, U., and Westhoff, M.: A thermodynamic
949 approach to link self-organization, preferential flow and rainfall-runoff behaviour,
950 Hydrology And Earth System Sciences, 17, 4297-4322, 10.5194/hess-17-4297-2013,
951 2013.
- 952 Zehe, E., Ehret, U., Pfister, L., Blume, T., Schroder, B., Westhoff, M., Jackisch, C.,
953 Schymanski, S. J., Weiler, M., Schulz, K., Allroggen, N., Tronicke, J., van Schaik, L.,
954 Dietrich, P., Scherer, U., Eccard, J., Wulfmeyer, V., and Kleidon, A.: Hess opinions:
955 From response units to functional units: A thermodynamic reinterpretation of the hru
956 concept to link spatial organization and functioning of intermediate scale catchments,
957 Hydrology And Earth System Sciences, 18, 4635-4655, 10.5194/hess-18-4635-2014,
958 2014.
- 959 Zhang, G. P., Fenicia, F., Rientjes, T. H. M., Reggiani, P., and Savenije, H. H. G.: Modeling
960 runoff generation in the geer river basin with improved model parameterizations to the
961 rew approach, Physics And Chemistry Of The Earth, 30, 285-296, 2005.
- 962 Zhang, L., Savenije, H. H. G., Fenicia, F., and Pfister, L.: Modelling subsurface strom flow
963 with the representative elementary watershed (rew) approach: Application to the alzette
964 river basin, HESSD-2005-0118, 2006.
- 965 Zhang, Z. L., and Savenije, H. H. G.: Thermodynamics of saline and fresh water mixing in
966 estuaries, Earth System Dynamics, 9, 241-247, 10.5194/esd-9-241-2018, 2018.
967